

Enzymatic DNA Synthesis by Engineering Terminal Deoxynucleotidyl Transferase

Xiaoyun Lu,[#] Jinlong Li,[#] Congyu Li, Qianqian Lou, Kai Peng, Bijun Cai, Ying Liu, Yonghong Yao, Lina Lu, Zhenyang Tian, Hongwu Ma, Wen Wang, Jian Cheng,* Xiaoxian Guo,* Huifeng Jiang,* and Yanhe Ma



Cite This: ACS Catal. 2022, 12, 2988–2997



Read Online

ACCESS |

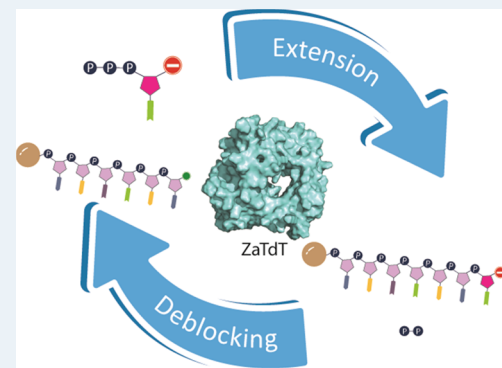
Metrics & More

Article Recommendations

Supporting Information

ABSTRACT: Template-free enzymatic approaches are considered the most promising solution for next-generation artificial DNA synthesis. However, the development of these technologies has been hampered by the lack of efficient enzymes specialized for stepwise nucleotide addition. By combining evolutionary analysis, high-throughput mutagenesis scanning, and rational design, we identified a terminal deoxynucleotidyl transferase from *Zonotrichia albicollis* (ZaTdT) and reshaped its catalytic cavity to better accommodate 3'-OH₂-modified nucleotides. The catalytic activity of the engineered ZaTdT for 3'-OH₂-dNTPs is 3 orders of magnitude higher than that of the commonly used mammalian TdT. The engineered ZaTdT enables highly efficient single-nucleotide extension of the growing oligonucleotide chain with an average stepwise yield of 98.7%, which makes it practical for *de novo* enzymatic DNA synthesis.

KEYWORDS: enzymatic DNA synthesis, terminal deoxynucleotidyl transferase (TdT), protein design, protein engineering, reversible terminator, deblocking



INTRODUCTION

As a promising technology, enzymatic DNA synthesis has been gaining interest since the 1950s.¹ Terminal deoxynucleotidyl transferase (TdT), one of the most promising DNA polymerases for *de novo* DNA synthesis, has been known to be able to incorporate random nucleotides into initiator strands in the absence of a template since the 1960s.^{2–6} However, the interest in developing enzymatic DNA synthesis declined after the successful establishment of the phosphoramidite method during the 1980s.^{7–9} In recent years, TdT has again attracted considerable attention due to the need for faster synthesis of longer DNA strands for data storage and synthetic biology.^{10–15} Since extensive studies have shown that TdT inherently incorporates several nucleotides within 1 s and can elongate the synthetic DNA to several kilobases,^{16–18} the superior synthesis length and speed are far beyond the reach of the commercially available phosphoramidite technology.^{19,20}

A wide variety of nucleotide analogues have been incorporated into DNA by TdT, which has enabled numerous applications,²¹ such as 3' end-labeling of DNA/RNA,^{22–24} immobilization of DNA,^{25,26} stabilization of DNA,^{27,28} conjugation of DNA to protein,^{29,30} and inspirational *de novo* synthesis of DNA.³¹ The major challenge in the application of TdT for the programmed synthesis of artificial DNA lies in controlling the polymerization of user-defined nucleotides.³² Several strategies have been designed to accomplish this. For

example, modulation of TdT extension to produce synthesized DNA capable of storing digital data has been experimentally demonstrated via management of reaction steps such as the degradation of the substrate and the release of divalent ion cofactors.^{33,34} Stringent control of TdT for single-nucleotide incorporation to synthesize DNA with precise sequences has been achieved using photocleavable TdT-dNTP conjugates.³⁵ Furthermore, reversible nucleotide terminators have been modified to control DNA synthesis.²¹ Among the functional modifications, reversible chemical moieties capping the 3'-OH group of the sugar unit have garnered great interest due to their better termination effect.³⁶ However, TdT has a relatively small active cavity, making it more difficult to incorporate sugar-modified nucleotides than natural nucleotides.^{37,38} The successful incorporation of sugar-modified nucleotides requires extensive engineering of TdT.^{39,40} Therefore, the implementation of a 3'-O-blocked reversible terminator and TdT for *de novo* DNA synthesis relies on the selection of a suitable blocking

Received: October 24, 2021

Revised: February 3, 2022

Published: February 18, 2022



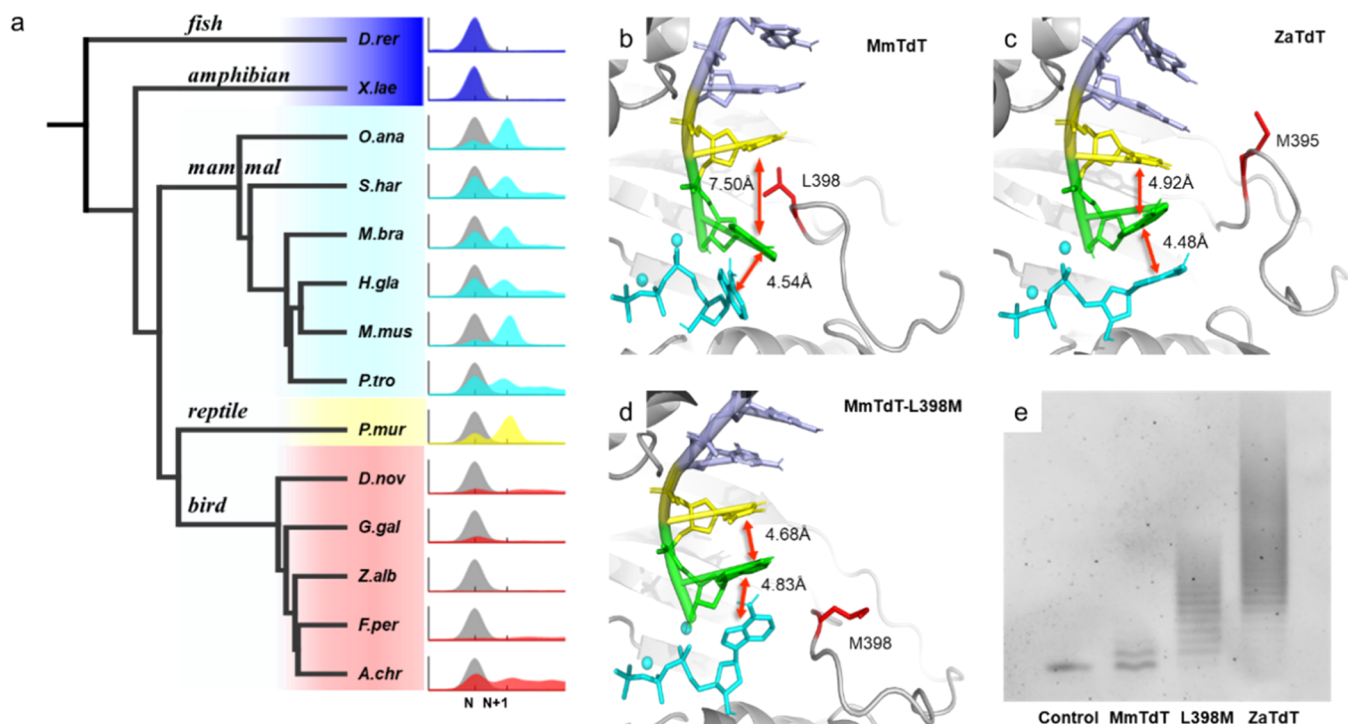


Figure 1. Polymerization activity of diverse TdT orthologs and structural features of TdT–substrate interactions. (a) Phylogenetic relationship of TdTs from representative vertebrates and characterization of the products of TdT-mediated primer extension reactions. Catalytic activity was evaluated by testing the extension of the 18 nt primer for 5 s. Reaction products were resolved by capillary electrophoresis (CE). The electropherograms colored in gray represents the control without TdT, and the electropherograms in other colors represents the reaction catalyzed by the corresponding TdT. N and N + 1 on the x-axes represent the retention times of 18 and 19 nt in the CE assay. Species list: *Danio rerio*, *Xenopus laevis*, *Ornithorhynchus anatinus*, *Sarcophilus harrisii*, *Myotis brandtii*, *Heterocephalus glaber*, *Mus musculus*, *Pan troglodytes*, *Podarcis muralis*, *Dromaius novaehollandiae*, *Gallus gallus*, *Z. albicollis*, *Falco peregrinus*, and *Aquila chrysaetos*. (b) Disruption of stacking between the bases (yellow and green) at the primer’s 3'-terminal dinucleotide by L398 in MmTdT. dATP and the last two bases are shown as cyan, green, and yellow sticks, respectively. Red lines indicate the corresponding base–base distance between two terminal bases and between the last 3' base and the incoming nucleotide (dATP). (c) ZaTdT accommodates base stacking interactions between the last two bases and the incoming nucleotide. (d) Substitution of L398M in MmTdT improved the base stacking interactions of terminal bases with the incoming nucleotide. (e) Denaturing polyacrylamide gel electrophoresis (PAGE) analysis of the primer extension reactions without enzyme (control), wild-type MmTdT, L398M variant of MmTdT, and ZaTdT.

group, engineering of TdT, and optimization of cycling conditions.

In this study, TdT orthologs from different vertebrates were selected for functional comparison, and a candidate with promiscuous catalytic activity was engineered to better accommodate 3'-ONH₂-modified nucleotides. The engineered TdT was then used to accurately synthesize a decamer oligonucleotide via an iterative single-nucleotide extension and deblocking cycle. This approach provides the possibility for enzymatic *de novo* DNA synthesis with quantitative coupling efficiencies comparable to the phosphoramidite process.

RESULTS

Catalytic Diversity among TdT Orthologs. Our knowledge regarding the structural features and physiological functions of template-independent DNA polymerases is primarily derived from molecular studies on mammalian TdT.^{37,38,41} The processivity of template-free nucleotide addition by TdTs derived from different species has remained elusive. Based on the phylogenetic tree of 137 TdT genes across the vertebrate taxa (Supporting Information Figure 1), we selected 14 TdTs from major clades of vertebrates including fish, amphibians, mammals, reptiles, and birds to test their catalytic activities in the incorporation of nucleotides into single-stranded initiators (Figure 1a). TdTs from different clades exhibited a

broad range of catalytic efficiencies with natural dNTPs. Remarkably, TdTs from birds incorporated multiple nucleotides into initiators, while other TdTs only incorporated one nucleotide into a small fraction of DNA initiators under the same conditions. Thus, avian TdTs enable faster polymerization of natural dNTPs. Moreover, ZaTdT from *Zonotrichia albicollis* had the highest polymerization activity among the tested TdTs.

To reveal the underlying mechanisms enabling the higher activity of ZaTdT, its structure was predicted using I-TASSER⁴² and AlphaFold2⁴³ (Supporting Information Figure 2). Due to the insertion of the Leu398 side chain in MmTdT (*Mus musculus* TdT), the last base at the 3'-terminus of the initiator strand is stacked with the incoming base (Figure 1b).³⁵ Surprisingly, the substitution of the corresponding residue with methionine in ZaTdT not only restored the dinucleotide stacking at the 3'-terminus but also slightly enhanced the base stacking interactions of the incoming dNTPs (Figure 1c). Substitution of Leu398Met in MmTdT also resulted in solvent exposure of Met398, which was consistent with the state of the corresponding residue in ZaTdT. This structure change reshaped the dinucleotide stacking at the 3'-terminus (Figure 1d), which ultimately led to an increased polymerization rate (Figure 1e). Taken together, our findings reveal an evolutionary innovation underlying the increased catalytic activity of avian TdT, which could be implemented to rationally design TdTs for higher catalytic activity.

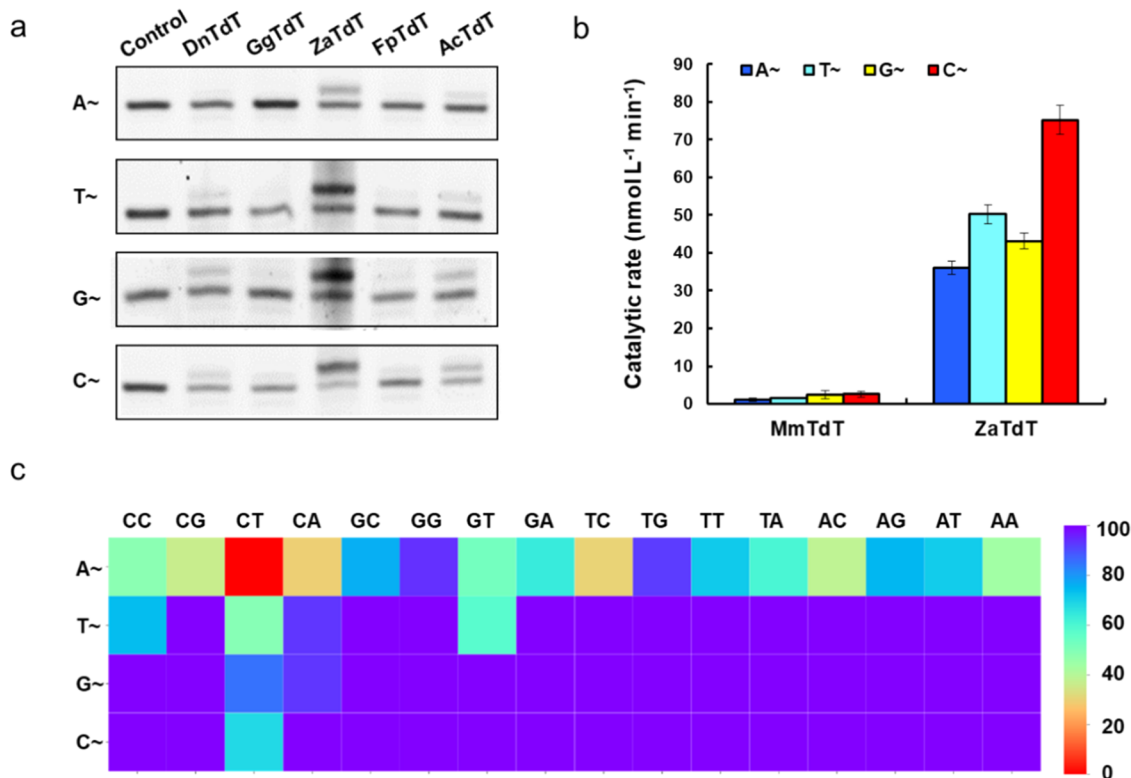


Figure 2. Incorporation of reversible terminator nucleotides by TdT. (a) Denaturing PAGE analysis of the incorporation of four 3'-ONH₂-blocked nucleotides by MmTdT and five avian TdTs. A~ = dATP-ONH₂; T~ = dTTP-ONH₂; G~ = dGTP-ONH₂; and C~ = dCTP-ONH₂. (b) Evaluation of the catalytic rates for the incorporation of four 3'-ONH₂-blocked nucleotides by MmTdT and ZaTdT. Next-generation high-throughput sequencing (NGS) was used to determine the product formation ratio (+1 extended initiator), and the catalytic rates were calculated as the rate of +1 product formation. Error bars represent the mean \pm SD of three replicates. (c) Heatmap of the quantification results of the single-nucleotide extension assays with ZaTdT and 16 initiators containing all possible dinucleotide combinations at their 3' end (rows) and four 3'-ONH₂-dNTPs (columns). Red to purple indicates the lowest to highest extension rate. The yields were calculated from the results of urea-PAGE shown in Supporting Information Figure 5.

Incorporation of Modified Nucleotides by ZaTdT. The strategy of employing TdT for DNA synthesis relies on the stepwise addition of desired nucleotides. This can be accomplished by adopting a reversible terminators, which stop the synthesis following the addition of each new nucleotide analogue. A wide range of sugar-modified nucleotide terminators have been successfully applied to pause nucleotide incorporation in DNA sequencing.^{36,44,45} To exploit the tolerance of TdT for sugar-modified nucleotides, 3'-ONH₂-dNTPs were used as substrates for avian TdTs because they carry a small blocking group compared to other sugar-modified nucleotides.⁴⁶ Polyacrylamide gel electrophoresis (PAGE) showed that ZaTdT displayed the highest efficiency in the incorporation of all 3'-ONH₂-blocked nucleotides (Figure 2a and Supporting Information Figure 3). To quantitatively measure the catalytic rates of ZaTdT, extension products were analyzed by next-generation sequencing. As shown in Figure 2b, the catalytic activities of ZaTdT with all 3'-ONH₂-dNTPs were about 18.0–34.8 times higher than those of MmTdT. In a comparison of the activity of ZaTdT with that of commercially available calf thymus TdT, ZaTdT exhibited higher activity (Supporting Information Figure 4). Given the higher catalytic rates with 3'-ONH₂-dNTPs, ZaTdT is a promising candidate for *de novo* DNA synthesis.

The base composition at the 3' end of the initiator strand is known to dramatically affect the incorporation efficiency of incoming nucleotides, especially the last two nucleotides, which

would interact with the incoming nucleotide through base stacking.⁴⁷ To examine the ability of ZaTdT to incorporate 3'-ONH₂-blocked nucleotides into different initiators, oligonucleotides terminated with 16 kinds of dinucleotides were extended with four types of 3'-ONH₂-blocked nucleotides (Figure 2c and Supporting Information Figure 5). All initiators exhibited a very low incorporation efficiency against 3'-ONH₂-dATP. In particular, the CT-terminated initiator showed no detectable extension with 3'-ONH₂-dATP. We found that there was only a relatively weak hydrogen bond (N–H–N) stabilizing the adenine base of 3'-ONH₂-dATP compared with other modified nucleotides (Supporting Information Figure 6), which significantly reduced the frequency of the precatalytic state (Supporting Information Figure 7 and Supporting Information Table 1). Similar reactions with the three other 3'-ONH₂-dNTPs for which complete extension of initiators terminated with dinucleotide variants were observed for all three 3'-ONH₂-dNTPs except for initiators terminated with CT, CC, CA, and GT (Figure 2c). By comparing the CT-terminated initiator with the other initiators, we found that the weaker base stacking is associated with a lower frequency of the prereaction state (Supporting Information Figures 8 and 9). It is possible that the weaker base stacking is more sensitive to the positioning of the incoming nucleotide. Therefore, the positioning of a 3'-ONH₂-modified nucleotide in ZaTdT not only altered the productive interactions with the active center of the polymerase but also

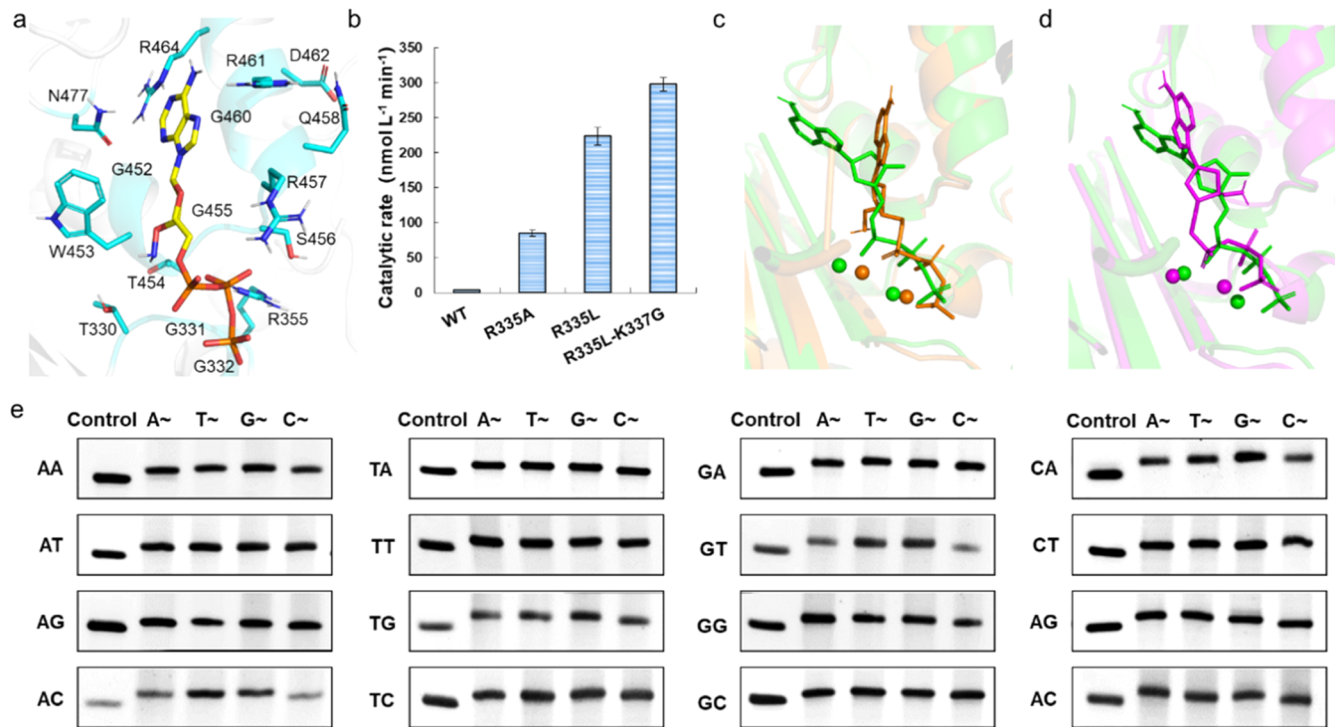


Figure 3. Engineering and rational designs of ZaTdT. (a) Residues (cyan sticks) within a 6 Å radius from the aminoalkoxyl group and base group of 3'-ONH₂-dATP in the wild-type ZaTdT. (b) Activity of ZaTdT mutants in the incorporation of 3'-ONH₂-dATP. (c) 3'-OH-dATP (green sticks) in ZaTdT aligned with 3'-ONH₂-dATP (orange sticks) in ZaTdT. Representative structures from MD simulations with different substrates docked into ZaTdT were selected. (d) Comparison of the docking pose of 3'-OH-dATP (green sticks) in the wild-type ZaTdT with 3'-ONH₂-dATP (magenta sticks) in the ZaTdT-R335L-K337G variant. Representative structures from MD simulations for the characterization of ZaTdT wild type and mutants were selected. (e) Denaturing PAGE analysis of double-mutant ZaTdT catalyzing the reactions of 16 initiators containing all possible dinucleotide combinations at their 3' end (rows) and four 3'-ONH₂-dNTPs (columns).

affected the base stacking interaction with the last two bases in the initiator.

Protein Engineering of ZaTdT. To make the active center more compatible with 3'-ONH₂-modified nucleotides, we attempted to reshape the catalytic cavity using two-site combinatorial mutagenesis on the residues within 6 Å around 3'-ONH₂ and the base moiety. After excluding residues implicated in interacting with the metal ions, the remaining residues were grouped according to their spatial positions at the modeled interaction surface between 3'-ONH₂ and ZaTdT. A total of 16 residues were divided into eight groups (Thr330-Gly331, Gly332-Arg335, Gly452-Trp453, Thr454-Gly455, Ser456-Arg457, Gln458-Gly460, Arg461-Asp462, and Arg464-Asn477) for mutagenesis screening (Figure 3a). To reduce codon redundancy and increase the efficiency of protein engineering, we designed degenerate codons based on the following criteria: (1) every amino acid is only encoded by one codon, (2) the wild-type amino acid at their original position must be included, and (3) as many as possible different side-chain types should be encompassed (i.e., hydrophobic-aliphatic, hydrophobic-aromatic, hydrophilic-polar uncharged, hydrophilic-acidic, and hydrophilic-basic). A total of 2160 clones from the mutant library were subjected to functional tests (Supporting Information Figure 10 and Table 2). Each mutant was individually purified for functional assessment *in vitro* to prevent mutants of ZaTdT from interference by endogenous nucleotides. Finally, all variants were examined for their ability to incorporate 3'-ONH₂-dAMP into an initiator terminated with the CT dinucleotide, which cannot be catalyzed at all by the wild-type ZaTdT.

Among the tested mutants, only Arg461Asp (R461D) and Arg335Ala (R335A) showed an increased in catalytic activity. ZaTdT-R461D exhibited an about 29-fold improvement in catalytic activity, which was attributed to the increased hydrogen-bond interactions with 3'-ONH₂-dAMP (Supporting Information Figure 11). However, this mutant had a significantly lower catalytic efficiency with other modified nucleotides (Supporting Information Figure 12). The mutant ZaTdT-R335A was also found to have significantly increased incorporation activity for 3'-ONH₂-dAMP. Although it exhibited a lower improvement (20-fold) in catalytic activity (Figure 3b), this mutant also displayed higher activity with other modified nucleotides compared to the wild-type ZaTdT (Supporting Information Figure 13).

Rational Design of ZaTdT Variants. To clarify the mechanisms through which the R335A substitution in ZaTdT affected its activity with 3'-ONH₂-dATP, we performed molecular dynamics (MD) simulations of the 3'-ONH₂-dATP docked into ZaTdT and ZaTdT-R335A. Analysis of the MD trajectories showed that R335 and its spatially neighboring residue K337 in ZaTdT contacted the triphosphate group through hydrogen bonds (Supporting Information Figure 14). The R335A substitution not only abolished the hydrogen-bond connection at position 335 but also reduced the frequency of hydrogen-bond formation between the triphosphate group and Lys337 from 84.1 to 32.7% (Supporting Information Figure 14). By evaluating other nonpolar side chains (Gly, Val, Ile, Leu, Met, Phe, Trp) at position 335 (Supporting Information Figure 15), we found that replacing arginine with leucine at position 335 would most extensively disrupt the hydrogen bonds between

K337 and the triphosphate moiety, leading to the lowest hydrogen-bonding frequency of 9.0% (*Supporting Information Figure 16*). Experimental assessment of the ZaTdT-R335L mutant revealed a 2.6-fold increase of 3'-ONH₂-dATP incorporation efficiency compared to ZaTdT-R335A (*Figure 3b*, *Supporting Information Figure 17*, and *Table 3*). The increased catalytic activity was caused by the lowering of the frequency of hydrogen-bond formation with the triphosphate moiety, which inspired us to create more freedom for the modified nucleotides.

To evaluate whether greater freedom of nucleotides could further increase the activity, K337 was mutated into Gly, Ala, Val, and Leu to completely eliminate the formation of hydrogen bonds between this site and the incoming nucleotide (*Supporting Information Figure 17*). Double-site variants combining K337G and R335L further resulted in an approximately 30% enhancement of the catalytic activity with 3'-ONH₂-dATP (*Figure 3b* and *Supporting Information Table 3*). The activity of the double-mutant ZaTdT-R335L-K337G was increased by 67.6-fold compared to the wild-type ZaTdT (*Figure 3b*). Taken together, the ZaTdT-R335L-K337G variant is approximately 1020-fold more efficient at incorporating 3'-ONH₂-modified nucleotides than the originally used MmTdT (*Supporting Information Figure 18*). Since 3'-ONH₂ occupies more space than 3'-OH, 3'-ONH₂-dATP exhibits positional changes inside ZaTdT due to steric hindrance (*Figure 3c*). The ZaTdT-R335L-K337G mutation releases constraints on the modified nucleotide and provides more space to accommodate 3'-ONH₂ so that the modified nucleotide assumes a conformation similar to that of the natural nucleotide (*Figure 3d*). Our PAGE analysis showed that the ZaTdT-R335L-K337G variant reacted almost completely with all tested initiators and all 3'-ONH₂-dNTPs (*Figure 3e*). Furthermore, we also found that Co²⁺ is the preferred metal cofactor for the incorporation of 3'-ONH₂ nucleotides (*Supporting Information Figure 19* and *Supporting Information Table 4*). A comparison of the kinetic parameters between the ZaTdT-R335L-K337G variant and wild-type ZaTdT further confirmed the improved catalytic efficiency of ZaTdT-R335L-K337G with 3'-ONH₂-dNTPs (*Table 1* and *Supporting Information Figure S20* and *S21*).

Table 1. Kinetic Parameters (K_m, k_{cat}, k_{cat}/K_m) for the Single-Nucleotide Incorporation Reaction^a

parameters	TdT variants	A~	T~	G~	C~
K _m [μM]	ZaTdT-WT	ND	42	16	81
	ZaTdT-R335L-K337G	1	2	15	4
k _{cat} [min ⁻¹]	ZaTdT-WT	ND	0.01	0.01	0.02
	ZaTdT-R335L-K337G	0.25	0.30	0.43	0.85
k _{cat} /K _m [M ⁻¹ s ⁻¹]	ZaTdT-WT	ND	2	11	3
	ZaTdT-R335L-K337G	3381	3166	473	3443

^a3'-ONH₂-dATPs without data (not determined: ND) were due to the inability to detect the product.

Template-Independent DNA Synthesis. To evaluate the performance of ZaTdT-R335L-K337G in *de novo* DNA synthesis from 3'-ONH₂-dNTPs, a two-step oligonucleotide synthesis cycle was adopted (*Figure 4a*). The initiator strands with a partial Illumina adapter sequence were preimmobilized onto magnetic beads via biotin-streptavidin chemistry. The initiators were extended with the desired nucleotide using

ZaTdT-R335L-K337G, followed by deblocking with buffered sodium nitrite to restore the free extendable 3'-OH. After 10 cycles of extension and deblocking, the cycling reaction products were extracted for dual-index paired-end sequencing analysis (*Figure 4b*). Sequences corresponding to the synthesized oligonucleotides were identified among the sequencing reads based on the up- and downstream tags (see the *Methods* section). After aligning to the target oligonucleotide sequence (5'-ATGACGTGCT-3'), approximately 70% of the sequences were identified to contain the full-length target sequence, while more than 25% had deletions of one or more nucleotides (*Figure 4c*). The high fraction of incomplete synthesis may have been caused by the sedimentation and clumping of beads. We noticed that a certain fraction of streptavidin beads formed aggregates with each other or the surface during the repeated separation process, which led to the clumps of beads becoming very difficult to resuspend upon removal of the magnet.

To avoid the formation of bead aggregates during the synthesis process, we tried to optimize the reaction system and the shaking method to reduce the electrostatic adsorption between the magnetic beads. After alleviating clump formation, we found that the yield for the complete desired oligonucleotides increased to 87.7% (691 779 of 789 003 reads) and the deletion rate decreased to 9.9% (*Figure 4c*). We further analyzed the yields of every individual cycle of the synthesis. As shown in *Supporting Information Figure 22*, the incorporation yield of the desired nucleotide in each cycle ranged from 99.4% (cycle 1) to 96.5% (cycle 10). Although the cycling reaction showed an increase of errors toward the end of synthesis, the stepwise yields were uniformly high for the six beginning cycles, thus ensuring a high level of average yield for all cycles (about $(0.877)^{1/10} = 98.7\%$). In summary, the two-step oligonucleotide synthesis strategy based on the ZaTdT-R335L-K337G variant and 3'-ONH₂-dNTPs has great potential for applications in *de novo* DNA synthesis.

DISCUSSION

Given the complexity of engineering protein–nucleotide interactions, protein engineering of TdT has been challenging in practice. In this study, the newly identified TdT of *Z. albibcollis* was tailored to enhance its catalytic activity with 3'-ONH₂-blocked nucleotides. The constraints on the 3'-ONH₂ nucleotides were relaxed by sequentially introducing the mutations R335A, R335L, and R335L-K337G, followed by a gradual increase of substrate dynamics, which allowed the equilibrium of the reaction to shift toward the efficient incorporation of 3'-ONH₂-dNTPs. By analyzing the binding modes of 3'-ONH₂-dATP in the ZaTdT-R335L-K337G variant, we found that the incoming 3'-ONH₂-dATP moved closer toward the initiator, while the γ-phosphate moiety of the 3'-ONH₂-dATP formed a new hydrogen-bonding interaction with R457 (*Supporting Information Figure 23*). Interestingly, mutations affecting R457 did not significantly change the catalytic efficiency of wild-type ZaTdT regardless of modification on the nucleotide substrates, while the same mutation significantly impaired the catalytic activity of ZaTdT-R335L-K337G (*Supporting Information Figures 24* and *25*). Thus, the hydrogen-bonding interaction with R457 not only stabilized the 3'-ONH₂-dATP but also established a new binding mode to push the 3'-ONH₂ moiety of 3'-ONH₂-dATP toward the position that was originally occupied by the 3'-OH moiety of dATP in the wild-type ZaTdT. Consequently, it overcame the incompatibility between 3'-ONH₂ nucleotides and the catalytic

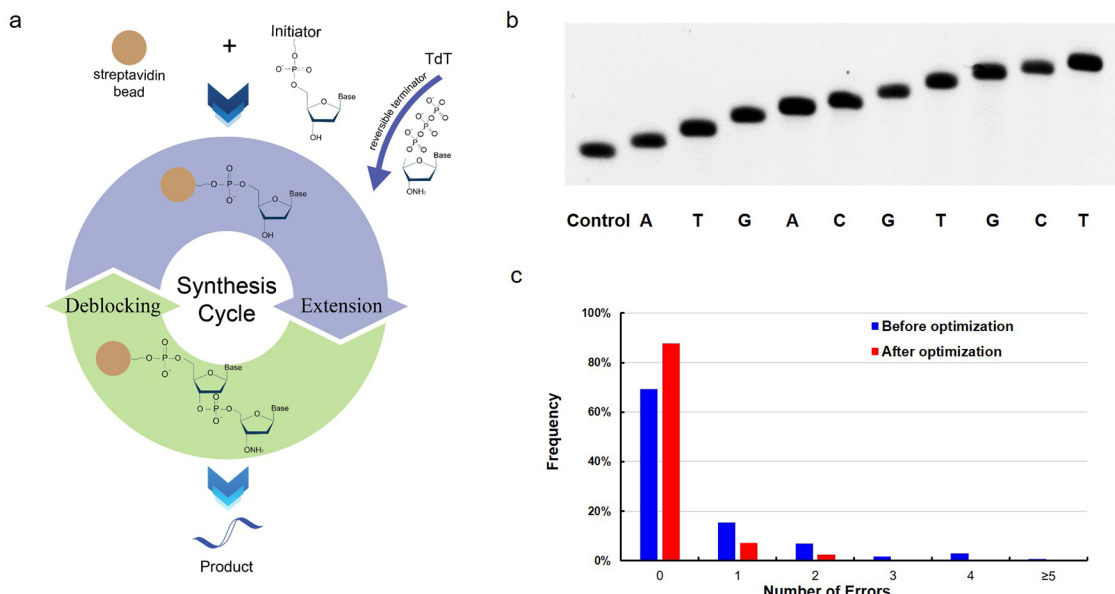


Figure 4. Utilization of engineered TdT in *de novo* DNA synthesis. (a) Two-step oligonucleotide synthesis cycle. The initiator strand with a partial adapter sequence was preimmobilized onto magnetic beads via biotin–streptavidin chemistry. The initiator was extended with desired nucleotides using the engineered ZaTdT, followed by deblocking with buffered sodium nitrite (pH 5.0) to restore the free extendable 3'-OH. (b) PAGE analysis of the 10 steps of extension in oligonucleotide synthesis. (c) Evaluation of the performance of our oligonucleotide synthesis strategy before and after process optimization. The x-axes refers to the number of deletions in synthetic oligonucleotides, where 0 represents completely correct synthesis.

cavity of ZaTdT. Thus, ZaTdT-R335L-K337G also showed a dramatic decrease of activity with natural deoxyribonucleotides and ribonucleotides compared with the wild-type ZaTdT (Supporting Information Figure 26). Our results are consistent with the notion that the generation of new reactions often requires breaking the original binding sites before reestablishing them in a different direction.⁴⁸

In our proof-of-concept study, although we improved the percentage of the complete desired oligonucleotides from 70 to 87.7% by preliminary optimization, we still observed approximately 9.9% deletions after 10 cycles of synthesis. Among them, 2.3% contained continuous deletions, which is significantly higher than the estimated frequency (less than 0.1%). The aggregation of magnetic beads was identified as the main cause. In addition to deletions, we also detected approximately 1.36% insertions and 1.03% substitutions after the 10 synthesis cycles (Supporting Information Figure 22). Theoretically, initiator strands cannot be extended beyond a single nucleotide due to the blocking of 3'-ONH₂ on the extended strands. Double-nucleotide addition is most likely caused by impurities in the stocks of reversible terminators. Additionally, substitutions may arise from the deamination of certain nucleobases by deblocking reagents.^{45,49} Careful adjustment of deblocking parameters must therefore be performed to further evaluate the impact of deblocking conditions. Although the current average stepwise yield of 98.7% may seem comparable with that of the commercialized chemical synthesis technology (99.5%),⁵⁰ it is important to acknowledge that even small differences in the stepwise yield dramatically affect the length of DNA that can be reliably synthesized. Hence, further optimization of the DNA synthesis system including but not limited to rational engineering of ZaTdT, optimization of the deblocking process, utilization of substrates with higher purity, and the integration of suitable solid supports such as silica-coated polymers are all necessary to make this system sufficiently efficient for *de novo* enzymatic DNA synthesis.

In summary, we used enzyme screening, protein engineering, and design to obtain the engineered ZaTdT with more than 1000-fold higher catalytic activity with 3'-ONH₂-dNTPs compared to the commonly used MmTdT. With improved understanding of the mechanisms underlying the changes in the catalytic activity of TdT, we believe that this enzyme could be tailored to accommodate other reversible terminators carrying photocleavable blocking groups to facilitate high-throughput automated DNA synthesis.

METHODS

Virtual Screening and Expression of TdT. By screening and comparing the TdT sequences in the NCBI database, 14 TdT genes from 14 vertebrates (mouse TdT gene was used as a reference) were synthesized for functional evaluation (Supporting Information Table 5). The details of virtual screening and phylogenetic analysis of TdT genes are shown in the Supporting Information. TdT genes were synthesized and cloned into a pET-28a vector between *Nde* I and *Xho* I (Supporting Information Table 6). TdT proteins were expressed in the *E. coli* BL21 (DE3) strain with the addition of IPTG. The expression and purification conditions of TdT proteins are shown in detail in the Supporting Information.

Functional Verification of TdTs. Catalytic activity of TdTs on natural nucleotides was determined in 30 μL reaction mixtures. The reaction system comprised 1 μM oligonucleotides (P1, Supporting Information Table 7), 0.1 mM dNTPs, 0.25 mM CoCl₂, 100 mM NaCl, and 50 mM phosphate buffer (pH 6.8). The catalytic reaction was started by adding 0.5 mg/mL purified protein. After incubation at 30 °C for 5 s, the reaction was stopped by heating at 95 °C. Products were analyzed by capillary electrophoresis (CE).

The catalytic reaction system for non-natural substrates comprised 1 μM oligonucleotides (P1), 0.25 mM 3'-ONH₂-dNTPs, 0.25 mM CoCl₂, 100 mM NaCl, and 50 mM phosphate buffer (pH 6.8). The catalytic reaction was started by adding 0.5

mg/mL purified protein. After incubation at 30 °C for 20 min, the reaction was stopped by heating at 95 °C. The products of the reaction were analyzed by polyacrylamide gel electrophoresis (PAGE).

Capillary Electrophoresis. Samples were assessed using a Qsep-400 automatic nucleic acid and protein analysis system (Bioptic, Taiwan, China). A disposable pen-shaped cartridge was inserted and other running buffers were loaded according to the manufacturer's instructions. The run was performed using a high-resolution cartridge with the sample injection protocol at 8 kV (kilovolts) for 10 s and separation at 6 kV for 300 s.

Polyacrylamide Gel Electrophoresis. Polyacrylamide gel electrophoresis was analyzed using 8 M urea and 20% acrylamide. Subsequently, the PAGE gel was stained with SYBR Gold nucleic acid gel dye for 20 min and scanned with a fully automatic fluorescence image analysis system (Tanon 5200, China). The result was processed with Gel Image System analysis software (Tanon, China), and the incorporation efficiency was calculated by dividing the initiator ($n + 1$) with one nucleotide added by the total initiator ($n + n + 1$).

Protein Engineering of ZaTdT. To obtain the desired saturation mutagenesis, oligonucleotide primers were designed with degenerate codons. In addition, each single-site saturation mutant was generated according to the PCR-based Quick-Change method. The PCR was performed according to the operation manual. The PCR product was digested with *Dpn*I restriction enzyme and transformed into BL21 (DE3) *E. coli* competent cells. An appropriate colony was used to express the mutant protein and verify its activity. Detailed instructions are given in the Supporting Information.

Molecular Dynamics Simulations. The initial DNA/nucleotide complex was constructed using the glide module⁵¹ based on PDB 4I27.⁴¹ The 3D complex models of mutants were built using Schrödinger software.⁵² AMBER18⁵³ was used for energy minimization of the constructed models, and molecular dynamics (MD) simulation of all of the models was performed using the ff14SB force field. The constrained MD simulations were conducted for 5 ns. Finally, 50 ns MD simulations were performed without any restriction except ions. The complete simulation methodology used in this work is available in the Supporting Information.

Extension of a DNA Strand by the Sequences 5'-ATGACGTGCT-3'. The 5' biotinylated oligonucleotide (P2, Supporting Information Table 7) immobilized on streptavidin magnetic beads was used for subsequent DNA synthesis. All nucleotide additions were performed at 30 °C for 10 min. Then, the products were treated with sodium nitrite buffer (700 mM, pH 5, adjust pH with nitrous acid) to cleave the ONH₂ group, generating a free 3'-OH group. For the 10 cycles of DNA synthesis, the modified nucleotides were used in the following order for the corresponding cycles: (1) 3'-ONH₂-dATP, (2) 3'-ONH₂-dTTP, (3) 3'-ONH₂-dGTP, (4) 3'-ONH₂-dATP, (5) 3'-ONH₂-dCTP, (6) 3'-ONH₂-dGTP, (7) 3'-ONH₂-dTTP, (8) 3'-ONH₂-dGTP, (9) 3'-ONH₂-dCTP, and (10) 3'-ONH₂-dTTP.

Sequencing Analysis of Synthesis Products. The 3' ends of the synthesized product were tailed with polyA using mouse TdT. Subsequently, the sequencing library was prepared for dual-index paired-end sequencing analysis in two steps. First, the polyA tailed products were amplified using common primers (C1, Supporting Information Table 7). Second, PCR was used to attach dual indices and Illumina sequencing adapters to the amplicons from the first-step PCR. PCRs were purified by DNA

Clean & Concentrator kit ("DCC", Zymo Research) and pooled for a shared 2 × 100 bp HiSeq (Illumina, San Diego, CA) run.

Evaluation of DNA Biosynthesis. The global and stepwise efficiency of DNA biosynthesis was calculated by a Perl script with the input of left-pair raw data of the "fastq" format. First, the sequences for all synthetic oligonucleotides were extracted from the sequencing reads by a pattern matching/AGTGCTACTAGGACGACTCGAATT(.*)?AAAAAAA/. Second, all extracted sequences were aligned to target the oligonucleotide sequence ATGACGTGCT. After alignment, the sequences were divided into four classes: the rightly synthetic sequences that are identical to target sequence, deletion-contained sequences (e.g., ATG-CGTGCT), insertion-contained sequences (e.g., ATGAACGTGCT), and substitution-contained sequences (e.g., ATGTCGTGCT). After classification, the synthetic errors in different locations were counted. Finally, the full-length yield was calculated by Nright/Nall, where Nright is the number of rightly synthetic sequences and Nall is the number of all extracted sequences. We further calculated the error rate resulted from continuous deletions by counting the deletion-contained sequences including at least one continuous gap and then dividing by the total number of sequences.

ASSOCIATED CONTENT

Supporting Information

The Supporting Information is available free of charge at <https://pubs.acs.org/doi/10.1021/acscatal.1c04879>.

Virtual screening and phylogenetic analysis of TdT genes; TdT expression and purification; incorporation of natural and modified nucleotides by TdT; molecular dynamics simulations; protein engineering of ZaTdT; functional verification of the reasonably designed ZaTdT variant; extension of a DNA strand by the sequences 5'-ATGACGTGCT-3'; sequence library preparation and next-generation sequencing analysis of synthesis products, and license description (note); phylogenetic tree of TDTs from 137 vertebrates (Figure S1); structure model of ZaTdT (Figure S2); incorporation of four 3'-ONH₂ reversible terminators by avian TdTs (Figure S3); catalytic efficiency of commercial calf thymus TdT and ZaTdT (Figure S4); denaturing PAGE analysis of single-nucleotide extension assay obtained from ZaTdT (Figure S5); hydrogen bond network between modified nucleotides and ZaTdT (Figure S6); hydrogen bonding of 3'-dATP263 and 3'-ONH₂-dTTP in ZaTdT (Figure S7); stacking state of different initiators in ZaTdT (Figure S8); percentage of precatalytic state of different nucleotide chains (Figure S9); iterative mutation and screening methods (Figure S10); hydrogen bonding interactions between base part of 3'-ONH₂-dTTP and residues R464, R461, or D461 (Figure S11); effect of R461D mutation on the catalytic efficiency of ZaTdT (Figure S12); effect of R355A mutation on the catalytic efficiency of ZaTdT (Figure S13); percentage of hydrogen bonding between triphosphate of 3'-ONH₂-dTTP and residues in position 335 and 337 during MD trajectories (Figure S14); effect of different mutations at position 335 on the proportion of hydrogen bonds at position 337 (Figure S15); percentage of hydrogen-bonding interaction between residues 335, 337, and 3'-ONH₂-dTTP with ZaTdT-R335L based on MD analysis (Figure S16); PAGE analysis of the activity

for different mutants (Figure S17); catalytic efficiency of different TdTs (Figure S18); enzyme kinetics of different metal ions (Figure S19); comparison of the kinetics for wild-type and mutant proteins (Figure S20); enzyme kinetics of different nucleotides for the wild-type ZaTdT (Figure S21); estimates of the stepwise yields of the synthesis based on an alignment against the target sequence (Figure S22); substrate binding conformation (Figure S23); effect of R457L mutation on ZaTdT activity (Figure S24); effect of R457L mutation on ZaTdT-R335L-K337G activity (Figure S25); and catalytic efficiency of wild-type and mutant protein on ribonucleotides (Figure 26); and frequency of pre-catalytic state for the incorporation of natural and modified nucleotides (Table S1); degenerate codons and their corresponding amino acid residues (Table S2); frequency of precatalytic state for the mutations in R335 and K337 (Table S3); kinetic parameters of ZaTdT-R335L-K337G variant influenced by four metal cofactors (Table S4); and TdT genes used in this study (Table S5) ([PDF](#))

AUTHOR INFORMATION

Corresponding Authors

Jian Cheng – National Center of Technology Innovation for Synthetic Biology, Tianjin 300308, China; Key Laboratory of Systems Microbial Biotechnology, Tianjin Institute of Industrial Biotechnology, Chinese Academy of Sciences, Tianjin 300308, China; Email: cheng_j@tib.cas.cn

Xiaoxian Guo – National Center of Technology Innovation for Synthetic Biology, Tianjin 300308, China; Key Laboratory of Systems Microbial Biotechnology, Tianjin Institute of Industrial Biotechnology, Chinese Academy of Sciences, Tianjin 300308, China; Email: guo_xx@tib.cas.cn

Huifeng Jiang – National Center of Technology Innovation for Synthetic Biology, Tianjin 300308, China; Key Laboratory of Systems Microbial Biotechnology, Tianjin Institute of Industrial Biotechnology, Chinese Academy of Sciences, Tianjin 300308, China;  orcid.org/0000-0002-3757-7896; Email: jiang_hf@tib.cas.cn

Authors

Xiaoyun Lu – National Center of Technology Innovation for Synthetic Biology, Tianjin 300308, China; Key Laboratory of Systems Microbial Biotechnology, Tianjin Institute of Industrial Biotechnology, Chinese Academy of Sciences, Tianjin 300308, China; School of Ecology and Environment, Northwestern Polytechnical University, Xi'an, Shanxi 710072, China; Zhonghe Gene Technology Co., Ltd., Tianjin 300308, China

Jinlong Li – National Center of Technology Innovation for Synthetic Biology, Tianjin 300308, China; Key Laboratory of Systems Microbial Biotechnology, Tianjin Institute of Industrial Biotechnology, Chinese Academy of Sciences, Tianjin 300308, China

Congyu Li – National Center of Technology Innovation for Synthetic Biology, Tianjin 300308, China; Tianjin University of Science & Technology, Tianjin 300457, China

Qianqian Lou – National Center of Technology Innovation for Synthetic Biology, Tianjin 300308, China; Key Laboratory of Systems Microbial Biotechnology, Tianjin Institute of Industrial Biotechnology, Chinese Academy of Sciences, Tianjin 300308, China

Kai Peng – National Center of Technology Innovation for Synthetic Biology, Tianjin 300308, China; Key Laboratory of Systems Microbial Biotechnology, Tianjin Institute of Industrial Biotechnology, Chinese Academy of Sciences, Tianjin 300308, China

Bijun Cai – National Center of Technology Innovation for Synthetic Biology, Tianjin 300308, China; Key Laboratory of Systems Microbial Biotechnology, Tianjin Institute of Industrial Biotechnology, Chinese Academy of Sciences, Tianjin 300308, China

Ying Liu – National Center of Technology Innovation for Synthetic Biology, Tianjin 300308, China; Key Laboratory of Systems Microbial Biotechnology, Tianjin Institute of Industrial Biotechnology, Chinese Academy of Sciences, Tianjin 300308, China

Yonghong Yao – National Center of Technology Innovation for Synthetic Biology, Tianjin 300308, China; Key Laboratory of Systems Microbial Biotechnology, Tianjin Institute of Industrial Biotechnology, Chinese Academy of Sciences, Tianjin 300308, China

Lina Lu – National Center of Technology Innovation for Synthetic Biology, Tianjin 300308, China; Key Laboratory of Systems Microbial Biotechnology, Tianjin Institute of Industrial Biotechnology, Chinese Academy of Sciences, Tianjin 300308, China

Zhenyang Tian – National Center of Technology Innovation for Synthetic Biology, Tianjin 300308, China; Key Laboratory of Systems Microbial Biotechnology, Tianjin Institute of Industrial Biotechnology, Chinese Academy of Sciences, Tianjin 300308, China

Hongwu Ma – National Center of Technology Innovation for Synthetic Biology, Tianjin 300308, China; Key Laboratory of Systems Microbial Biotechnology, Tianjin Institute of Industrial Biotechnology, Chinese Academy of Sciences, Tianjin 300308, China

Wen Wang – School of Ecology and Environment, Northwestern Polytechnical University, Xi'an, Shanxi 710072, China

Yanhe Ma – National Center of Technology Innovation for Synthetic Biology, Tianjin 300308, China; Key Laboratory of Systems Microbial Biotechnology, Tianjin Institute of Industrial Biotechnology, Chinese Academy of Sciences, Tianjin 300308, China

Complete contact information is available at:

<https://pubs.acs.org/10.1021/acscata.1c04879>

Author Contributions

[#]X.L. and J.L. contributed equally to this work. H.J., X.L., and X.G. designed the template-free DNA synthesis method. X.L., J.L., H.J., X.G., J.C., W.W., and Y.M. wrote the manuscript. X.L., C.L., and Q.L. contributed to the screening and directed evolution of ZaTdT. J.L. and H.M. contributed to the analysis of the enzyme's catalytic mechanism. X.L., K.P., B.C., and Y.L. performed the experiments of template-free DNA synthesis. Y.Y., L.L., and Z.T. prepared samples for NGS. J.C. contributed to NGS data analysis.

Notes

The authors declare the following competing financial interest(s): This work has been included in patent applications by Tianjin Institute of Industrial Biotechnology.

ACKNOWLEDGMENTS

This work was supported by the National Key R&D Program of China (2020YFC1316400), the National Science Fund for Excellent Young Scholars (31922047), the National Natural Science Foundation of China (31901015), and the Tianjin Synthetic Biotechnology Innovation Capacity Improvement Project (TSBICIP-KJGG-007 and TSBICIP-PTJS-002). The authors thank Yu Lei from Tianjin Institute of Industrial Biotechnology for her help with NGS.

REFERENCES

- (1) Sarac, I.; Hollenstein, M. Terminal Deoxynucleotidyl Transferase in the Synthesis and Modification of Nucleic Acids. *ChemBioChem* **2019**, *20*, 860–871.
- (2) Bollum, F. J. Thermal Conversion of Nonpriming Deoxyribonucleic Acid to Primer. *J. Biol. Chem.* **1959**, *234*, 2733–2734.
- (3) Bollum, F. J. Chemically Defined Templates and Initiators for Deoxypolynucleotide Synthesis. *Science* **1964**, *144*, 560.
- (4) Bollum, F. J. Calf Thymus Polymerase. *J. Biol. Chem.* **1960**, *235*, 2399–2403.
- (5) Grunberg-Manago, M.; Ortiz, P. J.; Ochoa, S. Enzymic Synthesis of Polynucleotides. I. Polynucleotide Phosphorylase of Azotobacter Vinelandii. *Biochim. Biophys. Acta* **1956**, *20*, 269–285.
- (6) Bollum, F. J. Oligodeoxyribonucleotide-Primed Reactions Catalyzed by Calf Thymus Polymerase. *J. Biol. Chem.* **1962**, *237*, 1945–1949.
- (7) Beauchage, S. L. aC.; M, H. Deoxynucleoside Phosphoramidites—a New Class of Key Intermediates for Deoxypolynucleotide Synthesis. *Tetrahedron Lett.* **1981**, *22*, 1859–1862.
- (8) Brown, D. M. A Brief History of Oligonucleotide Synthesis. *Methods Mol. Biol.* **1993**, *20*, 1–17.
- (9) Reese, C. B. Oligo- and Poly-Nucleotides: 50 Years of Chemical Synthesis. *Org. Biomol. Chem.* **2005**, *3*, 3851–3868.
- (10) Anavy, L.; Vaknin, I.; Atar, O.; Amit, R.; Yakhini, Z. Data Storage in DNA with Fewer Synthesis Cycles Using Composite DNA Letters. *Nat. Biotechnol.* **2019**, *37*, 1229–1236.
- (11) Ceze, L.; Nivala, J.; Strauss, K. Molecular Digital Data Storage Using DNA. *Nature reviews. Genetics* **2019**, *20*, 456–466.
- (12) Hutchison, C. A., 3rd; Chuang, R. Y.; Noskov, V. N.; Assad-Garcia, N.; Deerinck, T. J.; Ellisman, M. H.; Gill, J.; Kannan, K.; Karas, B. J.; Ma, L.; Pelletier, J. F.; Qi, Z. Q.; Richter, R. A.; Strychalski, E. A.; Sun, L.; Suzuki, Y.; Tsvetanova, B.; Wise, K. S.; Smith, H. O.; Glass, J. L.; Merryman, C.; Gibson, D. G.; Venter, J. C. Design and Synthesis of a Minimal Bacterial Genome. *Science* **2016**, *351*, No. aad6253.
- (13) Xie, Z. X.; Li, B. Z.; Mitchell, L. A.; Wu, Y.; Qi, X.; Jin, Z.; Jia, B.; Wang, X.; Zeng, B. X.; Liu, H. M.; Wu, X. L.; Feng, Q.; Zhang, W. Z.; Liu, W.; Ding, M. Z.; Li, X.; Zhao, G. R.; Qiao, J. J.; Cheng, J. S.; Zhao, M.; Kuang, Z.; Wang, X.; Martin, J. A.; Stracquadanio, G.; Yang, K.; Bai, X.; Zhao, J.; Hu, M. L.; Lin, Q. H.; Zhang, W. Q.; Shen, M. H.; Chen, S.; Su, W.; Wang, E. X.; Guo, R.; Zhai, F.; Guo, X. J.; Du, H. X.; Zhu, J. Q.; Song, T. Q.; Dai, J. J.; Li, F. F.; Jiang, G. Z.; Han, S. L.; Liu, S. Y.; Yu, Z. C.; Yang, X. N.; Chen, K.; Hu, C.; Li, D. S.; Jia, N.; Liu, Y.; Wang, L. T.; Wang, S.; Wei, X. T.; Fu, M. Q.; Qu, L. M.; Xin, S. Y.; Liu, T.; Tian, K. R.; Li, X. N.; Zhang, J. H.; Song, L. X.; Liu, J. G.; Lv, J. F.; Xu, H.; Tao, R.; Wang, Y.; Zhang, T. T.; Deng, Y. X.; Wang, Y. R.; Li, T.; Ye, G. X.; Xu, X. R.; Xia, Z. B.; Zhang, W.; Yang, S. L.; Liu, Y. L.; Ding, W. Q.; Liu, Z. N.; Zhu, J. Q.; Liu, N. Z.; Walker, R.; Luo, Y.; Wang, Y.; Shen, Y.; Yang, H.; Cai, Y.; Ma, P. S.; Zhang, C. T.; Bader, J. S.; Boeke, J. D.; Yuan, Y. J. "Perfect" Designer Chromosome V and Behavior of a Ring Derivative. *Science* **2017**, *355*, No. eaaf4704.
- (14) Mercy, G.; Mozziconacci, J.; Scolari, V. F.; Yang, K.; Zhao, G.; Thierry, A.; Luo, Y.; Mitchell, L. A.; Shen, M.; Shen, Y.; Walker, R.; Zhang, W.; Wu, Y.; Xie, Z. X.; Luo, Z.; Cai, Y.; Dai, J.; Yang, H.; Yuan, Y. J.; Boeke, J. D.; Bader, J. S.; Muller, H.; Koszul, R. 3D Organization of Synthetic and Scrambled Chromosomes. *Science* **2017**, *355*, No. eaaf4597.
- (15) Goldman, N.; Bertone, P.; Chen, S.; Dessimoz, C.; LeProust, E. M.; Sipos, B.; Birney, E. Towards Practical, High-Capacity, Low-Maintenance Information Storage in Synthesized DNA. *Nature* **2013**, *494*, 77–80.
- (16) Tjong, V.; Yu, H.; Hucknall, A.; Rangarajan, S.; Chilkoti, A. Amplified on-Chip Fluorescence Detection of DNA Hybridization by Surface-Initiated Enzymatic Polymerization. *Anal. Chem.* **2011**, *83*, S153–S159.
- (17) Tang, L.; Tjong, V.; Li, N.; Yingling, Y. G.; Chilkoti, A.; Zauscher, S. Enzymatic Polymerization of High Molecular Weight DNA Amphiphiles That Self-Assemble into Star-Like Micelles. *Adv. Mater.* **2014**, *26*, 3050–3054.
- (18) Tang, L.; Navarro, L. A., Jr.; Chilkoti, A.; Zauscher, S. High-Molecular-Weight Polynucleotides by Transferase-Catalyzed Living Chain-Growth Polycondensation. *Angew. Chem.* **2017**, *56*, 6778–6782.
- (19) LeProust, E. M.; Peck, B. J.; Spirin, K.; McCuen, H. B.; Moore, B.; Namsaraev, E.; Caruthers, M. H. Synthesis of High-Quality Libraries of Long (150mer) Oligonucleotides by a Novel Depurination Controlled Process. *Nucleic Acids Res.* **2010**, *38*, 2522–2540.
- (20) Kosuri, S.; Church, G. M. Large-Scale De Novo DNA Synthesis: Technologies and Applications. *Nat. Methods* **2014**, *11*, 499–507.
- (21) Jensen, M. A.; Davis, R. W. Template-Independent Enzymatic Oligonucleotide Synthesis (Tieos): Its History, Prospects, and Challenges. *Biochemistry* **2018**, *57*, 1821–1832.
- (22) Horáková, P.; Macíčková-Cahová, H.; Pivoňková, H.; Špaček, J.; Havran, L.; Hocek, M.; Fojta, M. Tail-Labeling of DNA Probes Using Modified Deoxynucleotide Triphosphates and Terminal Deoxynucleotidyl Tranferase. Application in Electrochemical DNA Hybridization and Protein-DNA Binding Assays. *Org. Biomol. Chem.* **2011**, *9*, 1366–1371.
- (23) Winz, M.-L.; Linder, E. C.; André, T.; Becker, J.; Jäschke, A. Nucleotidyl Transferase Assisted DNA Labeling with Different Click Chemistry. *Nucleic Acids Res.* **2015**, *43*, e110.
- (24) Rosemeyer, V.; Laubrock, A.; Seibl, R. Nonradioactive 3'-End-Labeling of RNA Molecules of Different Lengths by Terminal Deoxynucleotidyltransferase. *Anal. Biochem.* **1995**, *224*, 446–449.
- (25) Röhlisberger, P.; Levi-Acobas, F.; Sarac, I.; Baron, B.; England, P.; Marlière, P.; Herdewijn, P.; Hollenstein, M. Facile Immobilization of DNA Using an Enzymatic His-Tag Mimic. *Chem. Commun.* **2017**, *53*, 13031–13034.
- (26) Jakubovska, J.; Tauraitė, D.; Birštonas, L.; Meškys, R. N 4-Acyl-2'-Deoxycytidine-5'-Triphosphates for the Enzymatic Synthesis of Modified DNA. *Nucleic Acids Res.* **2018**, *46*, 5911–5923.
- (27) Kuwahara, M.; Obika, S.; Takeshima, H.; Hagiwara, Y.; Nagashima, J.-i.; Ozaki, H.; Sawai, H.; Imanishi, T. Smart Confering of Nuclease Resistance to DNA by 3'-End Protection Using 2', 4'-Bridged Nucleoside-5'-Triphosphates. *Bioorg. Med. Chem. Lett.* **2009**, *19*, 2941–2943.
- (28) Flamme, M.; Hanlon, S.; Iding, H.; Puentener, K.; Sladojevich, F.; Hollenstein, M. Towards the Enzymatic Synthesis of Phosphorothioate Containing Lna Oligonucleotides. *Bioorg. Med. Chem. Lett.* **2021**, *48*, No. 128242.
- (29) Ashley, J.; Schaap-Johansen, A.-L.; Mohammadniaei, M.; Naseri, M.; Marcatili, P.; Prado, M.; Sun, Y. Terminal Deoxynucleotidyl Transferase-Mediated Formation of Protein Binding Polynucleotides. *Nucleic Acids Res.* **2021**, *49*, 1065–1074.
- (30) Takahara, M.; Wakabayashi, R.; Minamihata, K.; Goto, M.; Kamiya, N. Primary Amine-Clustered DNA Aptamer for DNA-Protein Conjugation Catalyzed by Microbial Transglutaminase. *Bioconjugate Chem.* **2017**, *28*, 2954–2961.
- (31) Mathews, A. S.; Yang, H.; Montemagno, C. Photo-Cleavable Nucleotides for Primer Free Enzyme Mediated DNA Synthesis. *Org. Biomol. Chem.* **2016**, *14*, 8278–8288.
- (32) Minhaz Ud-Dean, S. M. A Theoretical Model for Template-Free Synthesis of Long DNA Sequence. *Syst. Synth. Biol.* **2008**, *2*, 67–73.
- (33) Lee, H. H.; Kalhor, R.; Goela, N.; Bolot, J.; Church, G. M. Terminator-Free Template-Independent Enzymatic DNA Synthesis for Digital Information Storage. *Nat. Commun.* **2019**, *10*, No. 2383.

- (34) Lee, H.; Wiegand, D. J.; Griswold, K.; Punthambaker, S.; Chun, H.; Kohman, R. E.; Church, G. M. Photon-Directed Multiplexed Enzymatic DNA Synthesis for Molecular Digital Data Storage. *Nat. Commun.* **2020**, *11*, No. 5246.
- (35) Palluk, S.; Arlow, D. H.; de Rond, T.; Barthel, S.; Kang, J. S.; Bector, R.; Baghdassarian, H. M.; Truong, A. N.; Kim, P. W.; Singh, A. K.; Hillson, N. J.; Keasling, J. D. De Novo DNA Synthesis Using Polymerase-Nucleotide Conjugates. *Nat. Biotechnol.* **2018**, *36*, 645–650.
- (36) Chen, F.; Dong, M.; Ge, M.; Zhu, L.; Ren, L.; Liu, G.; Mu, R. The History and Advances of Reversible Terminators Used in New Generations of Sequencing Technology. *Genomics, Proteomics Bioinf.* **2013**, *11*, 34–40.
- (37) Loc'h, J.; Rosario, S.; Delarue, M. Structural Basis for a New Templated Activity by Terminal Deoxynucleotidyl Transferase: Implications for V(D)J Recombination. *Structure* **2016**, *24*, 1452–1463.
- (38) Delarue, M.; Boule, J. B.; Lescar, J.; Expert-Bezancon, N.; Jourdan, N.; Sukumar, N.; Rougeon, F.; Papanicolaou, C. Crystal Structures of a Template-Independent DNA Polymerase: Murine Terminal Deoxynucleotidyltransferase. *EMBO J.* **2002**, *21*, 427–439.
- (39) Hollenstein, M.; Leumann, C. J. Synthesis and Biochemical Characterization of Tricyclothymidine Triphosphate (Tc-Ttp). *Chem-BioChem* **2014**, *15*, 1901–1904.
- (40) Sosunov, V. V.; Santamaría, F.; Victorova, L. S.; Gosselin, G.; Rayner, B.; Krayevsky, A. A. Stereochemical Control of DNA Biosynthesis. *Nucleic Acids Res.* **2000**, *28*, 1170–1175.
- (41) Gouge, J.; Rosario, S.; Romain, F.; Beguin, P.; Delarue, M. Structures of Intermediates Along the Catalytic Cycle of Terminal Deoxynucleotidyltransferase: Dynamical Aspects of the Two-Metal Ion Mechanism. *J. Mol. Biol.* **2013**, *425*, 4334–4352.
- (42) Yang, J.; Zhang, Y. I-Tasser Server: New Development for Protein Structure and Function Predictions. *Nucleic Acids Res.* **2015**, *43*, W174–181.
- (43) Jumper, J.; Evans, R.; Pritzel, A.; Green, T.; Figurnov, M.; Ronneberger, O.; Tunyasuvunakool, K.; Bates, R.; Žídek, A.; Potapenko, A.; Bridgland, A.; Meyer, C.; Kohl, S. A. A.; Ballard, A. J.; Cowie, A.; Romera-Paredes, B.; Nikolov, S.; Jain, R.; Adler, J.; Back, T.; Petersen, S.; Reiman, D.; Clancy, E.; Zielinski, M.; Steinegger, M.; Pacholska, M.; Berghammer, T.; Bodenstein, S.; Silver, D.; Vinyals, O.; Senior, A. W.; Kavukcuoglu, K.; Kohli, P.; Hassabis, D. Highly Accurate Protein Structure Prediction with AlphaFold. *Nature* **2021**, *596*, 583.
- (44) Guo, J.; Yu, L.; Turro, N. J.; Ju, J. An Integrated System for DNA Sequencing by Synthesis Using Novel Nucleotide Analogues. *Acc. Chem. Res.* **2010**, *43*, 551–563.
- (45) Hutter, D.; Kim, M. J.; Karalkar, N.; Leal, N. A.; Chen, F.; Guggenheim, E.; Visalakshi, V.; Olejnik, J.; Gordon, S.; Benner, S. A. Labeled Nucleoside Triphosphates with Reversibly Terminating Aminoalkoxyl Groups. *Nucleosides, Nucleotides Nucleic Acids* **2010**, *29*, 879–895.
- (46) Chen, F.; Gaucher, E. A.; Leal, N. A.; Hutter, D.; Havemann, S. A.; Govindarajan, S.; Ortlund, E. A.; Benner, S. A. Reconstructed Evolutionary Adaptive Paths Give Polymerases Accepting Reversible Terminators for Sequencing and Snp Detection. *Proc. Natl. Acad. Sci. U.S.A.* **2010**, *107*, 1948–1953.
- (47) Motea, E. A.; Berdis, A. J. Terminal Deoxynucleotidyl Transferase: The Story of a Misguided DNA Polymerase. *Biochim. Biophys. Acta* **2010**, *1804*, 1151–1166.
- (48) Renata, H.; Wang, Z. J.; Arnold, F. H. Expanding the Enzyme Universe: Accessing Non-Natural Reactions by Mechanism-Guided Directed Evolution. *Angew. Chem.* **2015**, *54*, 3351–3367.
- (49) McKenzie, L. K.; El-Khoury, R.; Thorpe, J. D.; Damha, M. J.; Hollenstein, M. Recent Progress in Non-Native Nucleic Acid Modifications. *Chem. Soc. Rev.* **2021**, *50*, 5126–5164.
- (50) Fearon, K. L.; Hirschbein, B. L.; Chiu, C. Y.; Quijano, M. R.; Zon, G., *Phosphorothioate Oligodeoxynucleotides: Large-Scale Synthesis and Analysis, Impurity Characterization, and the Effects of Phosphorus Stereochemistry*, Ciba Foundation Symposium, 1997; pp 19–31.
- (51) Schrödinger Release 2018-1: Glide; Schrödinger, Llc: New York, 2018. [Https://Www.Schrodinger.Com/Products/Glide](https://Www.Schrodinger.Com/Products/Glide) (Accessed 12 Sep, 2018).
- (52) Schrödinger Release 2018-1: Schrödinger, Llc: New York, Ny, 2018. [Https://Www.Schrodinger.Com/Products/Maestro](https://Www.Schrodinger.Com/Products/Maestro) (Accessed 12 Sep, 2018).
- (53) Case, D. A.; B-S, I. Y.; Brozell, S. R.; Cerutti, D. S.; Cheatham, T. E., III; Cruzeiro, V. W. D.; Darden, T. A.; Duke, R. E.; Ghoreishi, D.; Gilson, M. K.; Gohlke, H.; Goetz, A. W.; Greene, D.; Harris, R.; Homeyer, N.; Huang, Y.; Izadi, S.; Kovalenko, A.; Kurtzman, T.; Lee, T. S.; LeGrand, S.; Li, P.; Lin, C.; Liu, J.; Luchko, T.; Luo, R.; Mermelstein, D. J.; Merz, K. M.; Miao, Y.; Monard, G.; Nguyen, C.; Nguyen, H.; Omelyan, I.; Onufriev, A.; Pan, F.; Qi, R.; Roe, D. R.; Roitberg, A.; Sagui, C.; Schott-Verdugo, S.; Shen, J.; Simmerling, C. L.; Smith, J.; SalomonFerrer, R.; Swails, J.; Walker, R. C.; Wang, J.; Wei, H.; Wolf, R. M.; Wu, X.; Xiao, L.; York, D. M.; Kollman, P. A.. *Amber* 2018; University of California: San Francisco, <http://ambermd.org/>, 2018.

□ Recommended by ACS

Enzymatic Synthesis of DNA with an Expanded Genetic Alphabet Using Terminal Deoxynucleotidyl Transferase

Guangyuan Wang, Tingjian Chen, et al.

DECEMBER 01, 2022

ACS SYNTHETIC BIOLOGY

READ ▾

In Vitro Transcription/Translation-Coupled DNA Replication through Partial Regeneration of 20 Aminoacyl-tRNA Synthetases

Katsumi Hagino and Norikazu Ichihashi

APRIL 13, 2023

ACS SYNTHETIC BIOLOGY

READ ▾

A Nucleic Acid Sequence That is Catalytically Active in Both RNA and TNA Backbones

Dongying Wei, Hanyang Yu, et al.

OCTOBER 24, 2022

ACS SYNTHETIC BIOLOGY

READ ▾

Pyrococcus furiosus Argonaute Combined with Recombinase Polymerase Amplification for Rapid and Sensitive Detection of *Enterocytozoon hepatopenaei*

Lihong Yang, Song Gao, et al.

DECEMBER 22, 2022

JOURNAL OF AGRICULTURAL AND FOOD CHEMISTRY

READ ▾

Get More Suggestions >